5. Implemenation Package for a Drainage Blanket in Highway Pavement Systems. FHWA, U.S. Department of Transportation, May 1972.
6. M.Y. Shahin. Prediction of Low-Temperature and Thermal-Fatigue Cracking of Bituminous Pavements. Univ. of Texas, Austin, Ph.D. dissertation, Aug. 1972.
7. B.F. McCullough, A. Abou-Ayyash, W.R. Hudson, and J.P. Randall. Design of Continuously Reinforced Concrete Pavements for Highways. NCHRP, Project 1-15, 1975.
8. W.J. Kenis. Predicted Design Procedures--A Design Method for Flexible Pavements Using the VESYS Structural Subsystem. Proc., 4th International Conference on the Structural Design of Asphalt Pavements, Univ. of Michigan, Ann Arbor, Vol. 1, Aug. 1977.
9. J. Panak and H. Matlock. A Discrete-Element Method of Analysis for Orthogonal Slab and Grid Bridge Floor Systems. Center for Highway Research, Univ. of Texas, Austin, Res. Rept. 56-25, Aug. 1971.
10. H.J. Treybig, B.F. McCullough, P. Smith, and H. Von Quintus. Overlay Design and Reflection Cracking Analysis for Rigid Pavements--Volume 1: Development of New Design Criteria. FHWA, U.S. Department of Transportation, Final Rept. FHWA-RD-77-66, Jan. 1978.
11. E.S. Barber. Calculation of Maximum Pavement Temperatures from Weather Reports. HRB, Bull. 168, 1957, pp. 1-8.
12. R.E. Mills and R.F. Dawson. Fatigue of Concrete. HRB, Proc., Seventh Annual Meeting, 1928.
13. H.J. Treybig, M.F. McCullough, and W.R. Hudson. Tests of Existing Pavements and Synthesis of Design Methods. In CRC Airfield Pavements, U.S. Air Force Weapons Laboratory, Vol. 1, Dec. 1973.
14. W.R. Hudson and F.H. Scrivner. AASHO Road Test Principal Relationships--Performance with Stress, Rigid Pavements. HRB, Special Rept. 73, 1962, pp. 227-241.
15. A.S. Vesic and S.K. Saxena. Analysis of Structural Behavior of Road Test Rigid Pavements. NCHRP, Project 1-41(1), 1968.
16. The AASHO Road Test. HRB, Special Rept. 73, 1962.
17. P. Yimprasert and B.F. McCullough. Fatigue and Stress Analysis Concepts for Modifying the Rigid Pavement Design System. Center for Highway Research, Univ. of Texas, Austin, Res. Rept. 123-16, Jan. 1973.
18. K.D. Raithby and J.W. Galloway. Effects of Moisture Condition, Age, and Rate of Loading on Fatigue of Plain Concrete. In Abeles Symposium on Fatigue of Concrete, American Concrete Institute, Detroit, MI, ACI Publ. SP-41, 1974.
19. D.R. Snethen, L.D. Johnson, and D.M. Patrick. An Evaluation of Expedient Methodology for Identification of Potentially Expensive Soils. FHWA, U.S. Department of Transportation, Rept. FHWA-RD-77-94, June 1977.
20. P.D. Thompson, D. Croney, and E.W.H. Currer. The Alconbury Hill Experiment and Its Relation to Flexible Pavement Design. Proc., 3rd International Conference on the Structural Design of Asphalt Pavements, London, England, Sept. 1972.
21. Fatigue-Coverage Concepts Applied to Concrete Airport Pavement Designs. Portland Cement Association, Skokie, IL, Tech. Paper, 1973.
22. M.I. Darter and E.J. Barenberg. Zero-Maintenance Pavement: Field Studies on the Performance Requirements and Capabilities of Conventional Pavement Systems. FHWA, U.S. Department of Transportation, Rept. FHWA-RD-76-105, April 1976.
23. N.W. Lister and C.K. Kennedy. A System for the Prediction of Pavement Life and Design of Pavement Strengthening. 4th International Conference on the Structural Design of Asphalt Pavements. Univ. of Michigan, Ann Arbor, Vol. 1, Aug. 1979.
24. Local Climatological Data: Annual Summaries for 1977, Parts 1 and 2. National Oceanic and Atmospheric Administration, National Climatic Center, Asheville, NC, 1977.
25. AASHTO Interim Guide for Design of Pavement Structure 1972. AASHTO, Washington, DC, 1974.
26. The AASHO Road Test: Report 5--Pavement Research. HRB, Special Rept. 61E, 1962.

Publication of this paper sponsored by Committee on Pavement Rehabilitation Design.

Model Study of Anchored Pavement

SURENDRA K. SAXENA AND S.G. MILISOPOULOS

A laboratory model study of an anchored pavement is described. The objective of the study was to investigate construction problems and development of specifications for a full-scale test. Also, the model tests could be and have been used to verify the analytical model. The model pavement involved 1/20-scale anchored and conventional slabs of similar dimensions and made of aluminum, a subgrade of known properties, a container tank for the whole setup, and loading and measuring equipment. In addition, one set of tests was performed by using the anchored slab in such a way that it is not in contact with the subgrade. The open space (void) between the slab and the subgrade simulates the worst conditions of no support caused by high moisture in the subgrade due to thaw or other actions. The model test results were compared with results from finite-element analysis. The investigations confirm that an anchored slab offers distinct advantages over a conventional slab; for example, the deflections are lower and uniform compared with those from a conventional slab, and stresses in the soil are reduced and distributed more widely by rigid anchors. The ANSYS computer program can analyze such a soil-structure system and incorporate the environmental and mechanical effects.

Serious concern about the maintenance costs and agonizing delays in repairs of highways in highly urban areas raised the question of the feasibility of designing and constructing minimum-maintenance pavements. As a result of research sponsored by the Federal Highway Administration, several structural concepts have been proposed (1) for minimum-maintenance performance. These include pile support, edge stiffening, thick cellular systems, waffle-type systems, modified conventional systems, and a flex-

Figure 1. Configuration of conventional and anchored pavements studied.

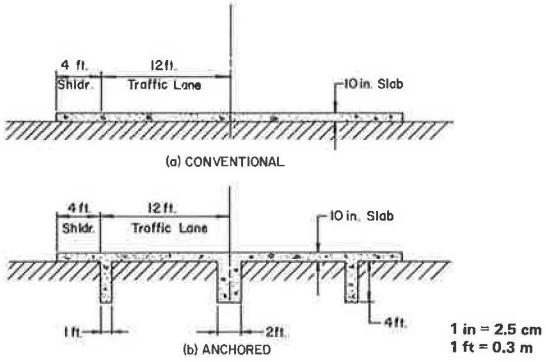

Figure 2. Views of ASL 62 in long.

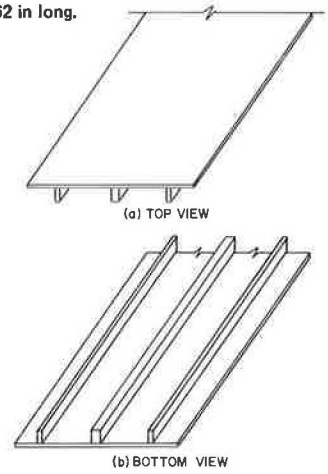

Figure 3. Plan view of testing tank and sampling tank.

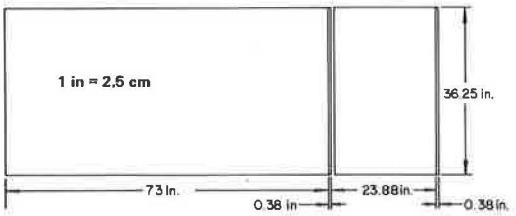

Figure 4. Loading platform: (a) plan view and (b) cross section.

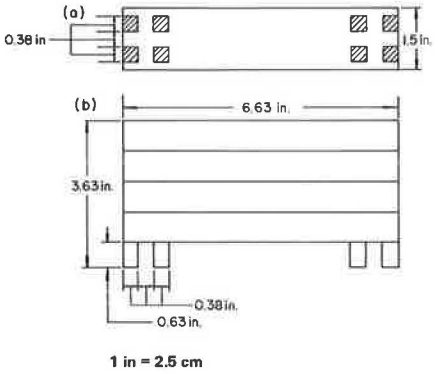

Figure 5. Cross section of ASL.

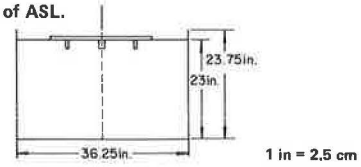

ible "floating" V-shaped pavement. A limited study of various concepts showed an anchored pavement (Figure 1) to be promising because it uses a similar amount of structural material as current systems do, does not pose great construction difficulties, and may require little subgrade preparation. A laboratory model study of the anchored pavement is reported in this paper. The objective of the model study was twofold: first, to verify the results of the analytical model (computer program) and, second, to investigate construction problems and help to develop specifications for a full-scale test.

Experimental investigations of the structural behavior of rigid pavements have been made in the past at Arlington Experimental Farm in Virginia (2) and at Iowa State Engineering Experimental Station (3). Full-scale tests were performed at Schiphol Airport in Holland (4) and on Interstate 80 near Ottawa, Illinois, as part of the AASHO Road Test Program (this last test generated many studies). Model tests were performed under controlled conditions by Vesic and Saxena (5) to study the effect of stress due to load alone.

MODEL TESTS AND INSTRUMENTATION

The model tests for this investigation were 1/20 scale and involved anchored and conventional aluminum slabs of similar lengths, a subgrade of known properties, a container tank for the soil and for conducting the experiment, and loading and measuring equipment.

Slabs

Both the anchored and the conventional slabs were 62 in (157.5 cm) long, 21.63 in (55 cm) wide, and 0.5 in (1.27 cm) deep. For the anchored slab, there was an anchor near each edge and a central anchor. The two edge anchors measured 1.88 in (4.8 cm) deep and 0.625 in (1.6 cm) wide. The central anchor had the same depth but was 1.25 in (3.2 cm) wide. The lengths of the anchors and the slab were obviously the same. The anchors were attached to the slab by screws centered at 5 in (12.7 cm). Figure 2 shows the top and bottom views of the anchored pavement.

Subgrade and Container

The subgrade used was a soil made up of 42 percent kaolinite clay, 42 percent silica sand, and 16 percent water by weight. The subgrade was classified as silty clay that had a plasticity index of 16 and an optimum water content of about 8 percent. The soil was mixed with an over-the-optimum water content of 16 percent. A soil mixer and a compactor were used to prepare the subgrade. The silty-clay subgrade was mixed in 100-lb (45.36-kg) batches and then deposited in the tank, which was divided into two areas, testing and sampling (Figure 3). The testing area was 73 in (185.4 cm) deep. The sampling area was 27.88 in (70.8 cm) long; the other dimensions were the same. The subgrade was compacted in 2-in (5.08-cm) layers. For a uniform compaction, two passes of the compactor per layer were found to be sufficient. Before another layer was placed, the top 0.5 in (1.27 cm) of the previous layer was raked to ensure a proper bond. Every effort was made to have uniform compaction in all layers. The uppermost layer was leveled with

Figure 6. Positions of load, dial gages, and surface deflections.

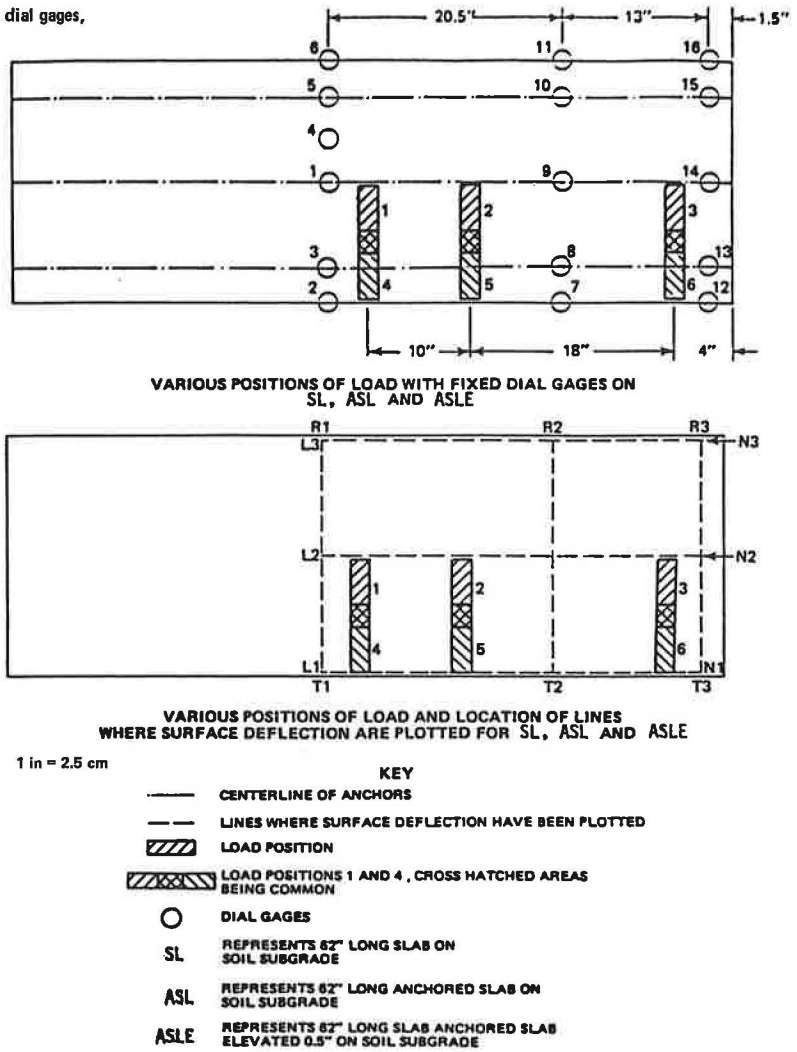

Figure 7. Positions of dial gages on ASL.

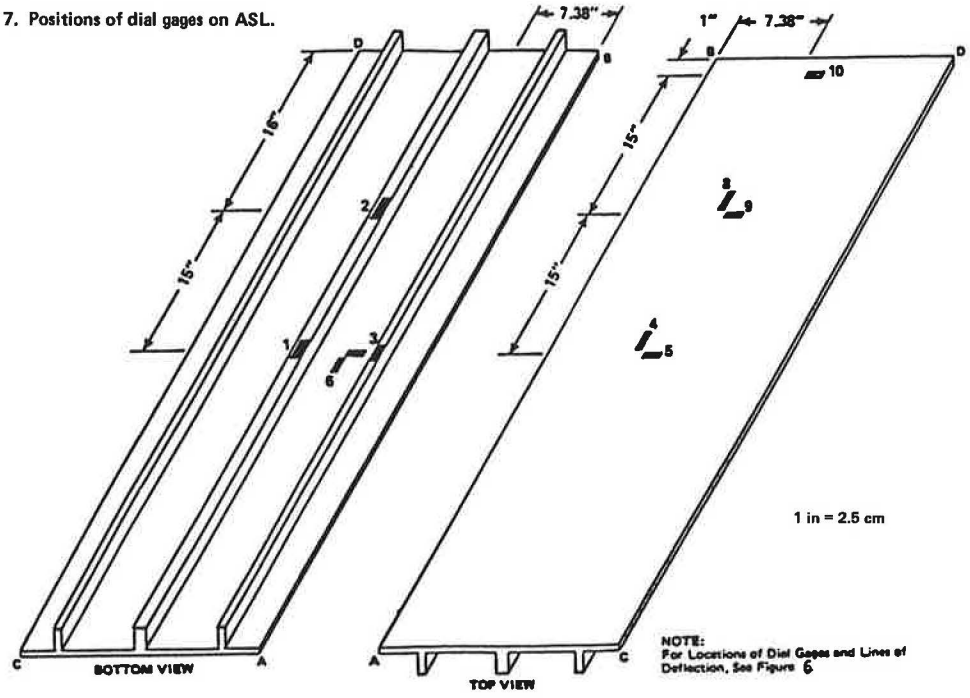

Figure 8. Load at center of ASL (traffic lane).

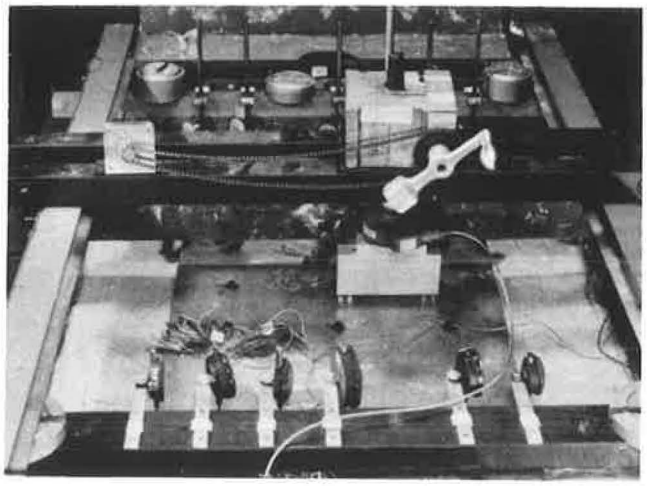

Figure 9. (a) Longitudinal and (b) transverse surface deflections along lines L2-N2 and T1-R1, load position 1, for ASL and SL.

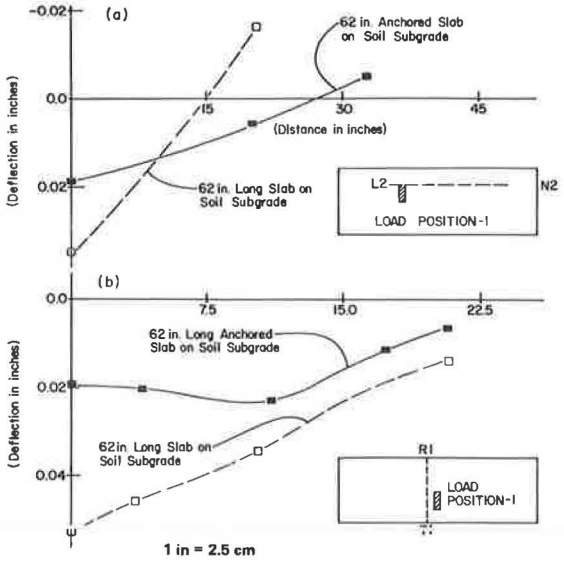

precision to ensure proper contact between the slab and the subgrade. When the anchored system was used, anchors were placed before the leveling of the upper layer; then, after leveling, the slab was screwed to them. To avoid disturbing the soil, this method was considered better than welding the anchors to the plate. Crossbars were used to keep the anchors in position during compaction; the crossbars were removed later.

The properties of the subgrade were measured by performing many tests on undisturbed specimens obtained from the sampling area and by a plate-load test performed in situ. An odometer-type K_o-test provided an overconsolidation ratio of 30 and a value of K_o equal to 2.6. The observed value of K_o is in agreement with that in the published literature for overconsolidated clays (6) and compacted clays (7). The consolidated undrained triaxial tests provided a value of cohesion intercept $\bar{c}$ = 200 lbf/in² (9.58 kN/m²) and angle of interval friction $\bar{\phi}$ = 18°. The plate-load tests provided a secant mold of 850 lbf/in² (5865 kN/m²). The Poisson ratio adopted was ν = 0.4. The mold of elasticity of the aluminum slab was 10.5 x 10⁶ lbf/in² (72.45 x 10⁶ kN/m²).

Loading and Measuring Equipment

The loading platform (Figure 4) was designed to represent a 1/20-scale model of two rear-axle trucks that have four tires per axle and a maximum capacity of 18 000 lb (8165 kg) per axle. The 18 000-lb/axle load on a 1/20 scale was equal to a 45-lb (20.4-kg) load; however, heavier loads were used within the elastic range to investigate the response of the slab-subgrade system. For load application, a manual jack that had an attached load cell was used. A strain-indicator unit and balance unit were used to measure the strains of 10 foil strain gages fixed at various locations on the slab. The following notation was used for the test series.

1. Anchored slab, 62 in, laid on soil subgrade--ASL;
2. Conventional slab, same length, on soil subgrade--SL; and
3. Anchored slab, same length, elevated by 0.5 in from soil subgrade--ASLE.

TEST DETAILS

Anchored Slab on Soil Subgrade (ASL)

A cross-sectional view of the ASL is shown in Figure 5. The positions of the dial gages for measuring surface deflections of the anchored slab are shown in Figure 6. The 16 numbered points at which the deflections were measured were used to draw transverse and longitudinal deflections along sections T1-R1, T2-R2, and T3-R3 and along sections L1-N1, L2-N2, and L3-N3, respectively (Figure 6). Ten dial gages were placed on the slab to measure strain and deduce the stress and bending movement. Five dial gages were placed on the top surface of the slab, two on the bottom surface, and the other three on the anchors (Figure 7).

A line preloading was initially used at the center, quarter distances, and edges of the anchored slab. The preloading was considered necessary to ensure contact between the slab and the soil and also to bring the soil within elastic range. It was found that after about five loading and unloading cycles, the soil was within elastic range. As shown in Figure 6, six load positions were used to investigate the response of a continuous pavement and that of a pavement at a joint that has zero transfer load. The load was applied in increments of 250 lb (113.4 kg). Although the applied maximum load was 1500 lb (680.4 kg), the plots in the paper only show deflection for 250-lb, 500-lb (227-kg), and 750-lb (340-kg) loads. Figure 8 shows one of the various loading configurations, and Figures 9 and 10 show longitudinal and transverse deflections at centerlines (L2-N2 and T1-R1) for load at positions 1 and 3 only.

Conventional Slab on Subgrade (SL)

Deflections were measured at the same 16 locations shown in Figure 6. Six dial gages were attached to the top of the slab and four were attached to the bottom. After preloading in the center, at the left, and at the right intermediate sections, regular loading was applied. A maximum load of 750 lb that had a load increment of 250 lb was used at six loading positions (Figure 6). The deflections are shown with the anchored-slab deflections for only two loading positions.

Figure 10. (a) Longitudinal and (b) transverse surface deflections along lines L2-N2 and T1-R1, load position 3, for ASL and SL.

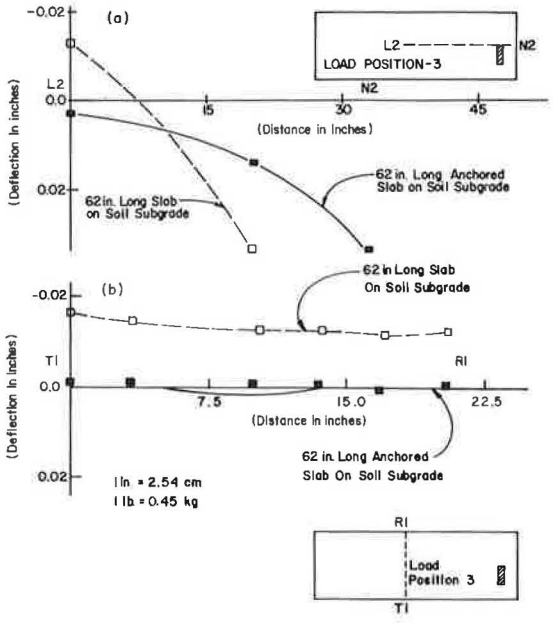

Figure 11. Cross section of ASLE.

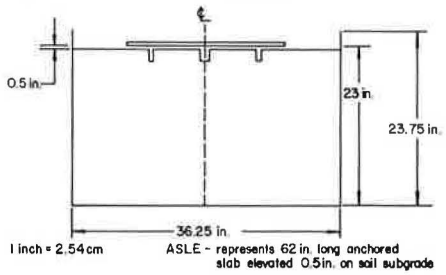

Figure 12. ASLE experimental set-up.

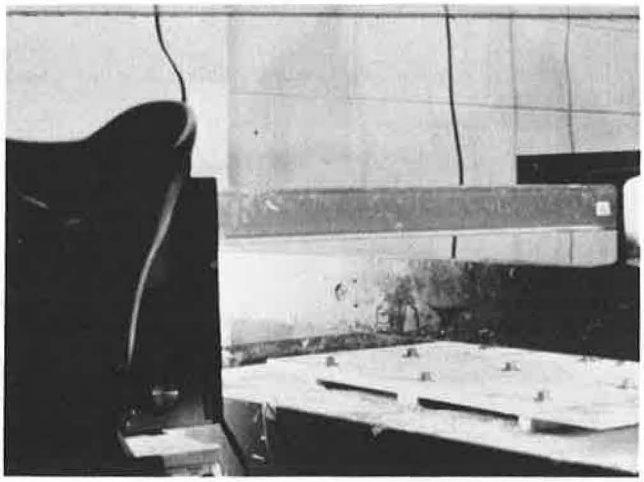

Elevated Anchored Slab (ASLE)

The procedure was similar to that for previous experiments. Before the slab was screwed to the anchors, a 0.5-in (1.27-cm) space was left between the slab and the subgrade. The space simulates the worst conditions of no-support capability caused by high moisture in the subgrade due to thaw or other action. Figure 11 shows a cross section of the model, and Figure 12 is a view of the experimental set-up. Preloading was done at the center, at the quarter distance on the left, at the quarter distance on the right, and near the edge on the left and the right to bring the soil into elastic range. The preloading was done symmetrically to avoid any possible lifting of the anchored slab. After preloading, the slab was loaded at six positions as described before. The maximum load applied was 300 lb (136 kg) in increments of 100 lb (45.36 kg). The load being applied to the subgrade at concentrated points had to be low enough not to cause plastic (or bearing-capacity-type) failure. Figures 13 and 14 show longitudinal and transverse deflections for the middle section only for load positions 1 and 3.

TEST RESULTS

The surface deflections of the anchored slab in the longitudinal direction and the central transverse section for the central loading position (position 1) are about one-third of those obtained for a conventional slab. At the quarter distance from the edge and near the edge, the conventional slab exhibited significant uplifting, whereas the anchored slab had almost no uplift or insignificant uplift only at the edge. Similar trends--that is, differential magnitudes of the order of one-third--were observed for the edge loading (position 3), as shown in Figure 10. The uplifting of the center was very pronounced for the conventional slab but insignificant for the anchored slab (Figures 9a and 10b). The anchored slab was also compared with the elevated-slab system. The surface deflections beneath the load for position 1 of the anchored slab are about one-third to two-thirds of the deflections for the elevated slab. No significant uplifting was observed in the elevated slab. The experiments indicate clearly that for a load of 250 lb only, the deflections of the anchored slab in full contact (Figures 13 and 14) and those of the elevated pavement were found to be very similar. This shows that a considerable amount of load is carried by anchors to the soil beneath.

ANALYTICAL SOLUTION

The analytical solution uses the options available in computer program ANSYS. In this section a comparison of anchored pavement with the conventional slabs and with the elevated anchored slab (which represents loss of contact below the slab) is presented.

Eight-node brick elements were used in the finite-element analysis (three-dimensional analysis). In case of the ASL and the conventional slab (SL), interface elements of infinitesimal length were used between the slab and the subgrade soil. Thus the effect of the uplifting, when the slab loses contact with the subgrade soil, was taken into account.

SIMPLY SUPPORTED SLABS

To verify the computer program, analyses of a simply supported anchored slab (SASL) and a simply supported conventional slab (SSL) were performed first and compared with experimental results. In the experiment, a line load of 2.95 lbf/in^2 (20.36 kN/m^2) was applied 1 in from the transverse centerline. The longitudinal deflections at the centerline are plotted in Figure 15, which shows the experimental deflection, the deflection obtained by

Figure 13. (a) Longitudinal and (b) transverse surface deflections along lines L2-N2 and T1-R1, load position 1, for ASL and ASLE.

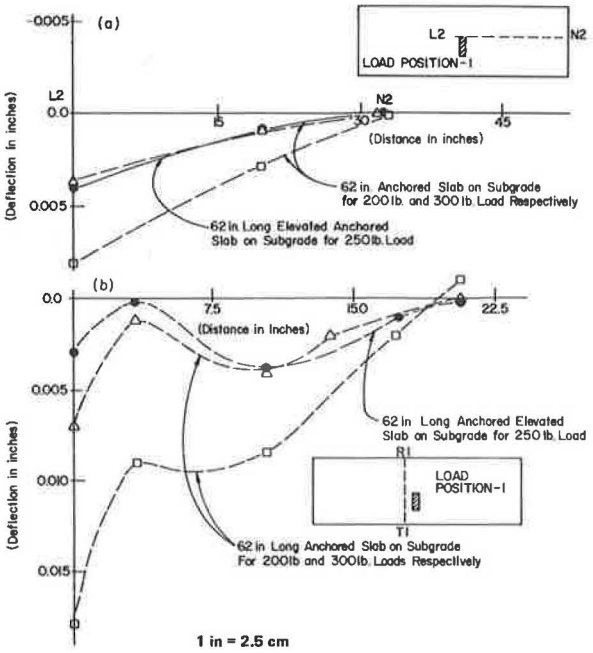

Figure 14. (a) Longitudinal and (b) transverse surface deflections along lines L2-N2 and T1-R1, load position 3, for ASL and ASLE.

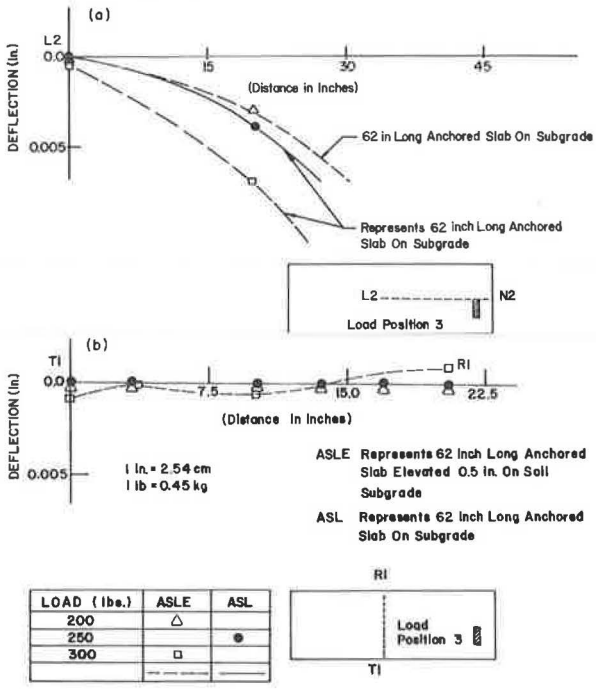

the finite-element method, and that obtained by the beam theory. The difference between the results from the finite-element method and the experimental values is about 7 percent for the SASL and about 4.5 percent for the SSL. The difference between the beam-theory approach and the experimental work is about 8.5 percent for both cases. Figure 16 shows the longitudinal deflections at the centerline of the SASL and the SSL by using the finite-element method. The intent is to demonstrate clearly the effect of the additional rigidity of the anchored

Figure 15. Longitudinal deflections at center for comparison of experimental, finite-element, and beam-theory models.

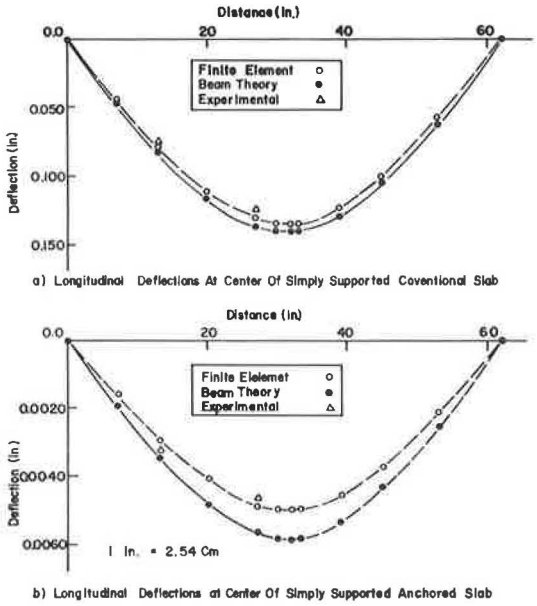

Figure 16. Longitudinal deflections at center for comparison of finite-element models of SSL and SASL.

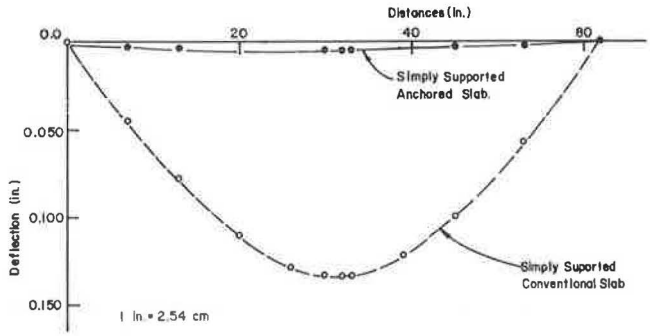

Figure 17. Vertical stress and strain contours for 750-lb load, position 1, for SL.

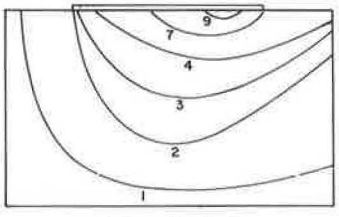

1 lbf/in^2 = 0.07 kg/cm^2

(a) Vertical Stress Contours.

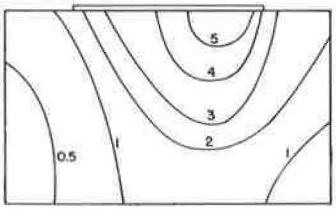

1 Micro .In./In. =0.001 cm/cm

(b) Vertical Strain Contours.

Figure 18. Vertical stress and strain contours for 750-lb load, position 1, for ASL.

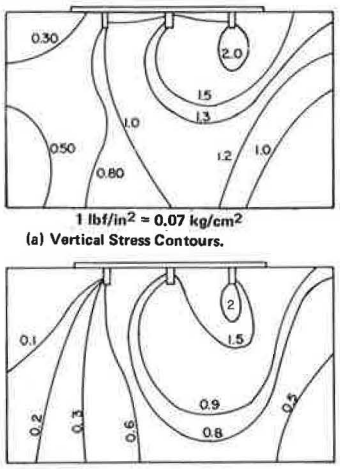

Figure 19. Vertical stress and strain contours for 200-lb load, position 1, for ASLE.

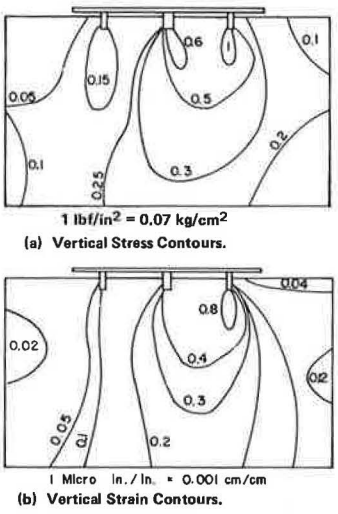

Figure 20. Transverse surface deflections along line T1-R1, load position 1, for SL.

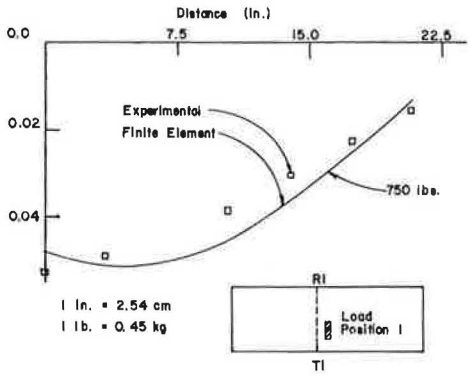

slab compared with that of the conventional slab.

The finite-element models for the ASL, the SL, and the ASLE are described by Saxena, Hedberg, and Ladd (6). For analytical investigation, a 750-lb load was applied at position 1 (see Figure 6) on the ASL and the SL, whereas a load of only 200 lb (90.72 kg) was applied at the same position for the ASLE. The vertical stress and strain contours only are presented for the three cases in Figures 17, 18, and

Figure 21. Transverse and longitudinal surface deflections along lines T1-R1 and L2-N2, load position 1, for ASL.

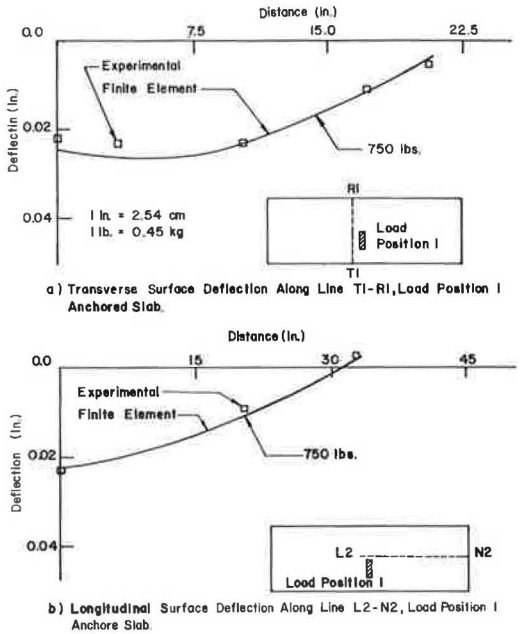

19. In the case of the SL, a maximum stress of 9 lbf/in² (62.1 kN/m²) and a maximum strain of 0.005 in/in (0.013 cm/cm) underneath the load was observed. The analytical results also indicate a maximum deflection of 0.1 in (2.54 cm) under the load, and more than half of the slab loses contact with the subgrade with maximum uplift of 0.012 in (0.30 mm) (1).

For the ASL, a maximum stress of only 2 lbf/in² (13.8 kN/m²) and a maximum strain of 0.002 in/in (0.030 cm/cm) underneath the right anchor was observed. The analytical results indicate a maximum deflection of 0.031 in (0.8 mm) in the right anchor (closest to the load) and almost no serious uplift of the anchors except at the left and right edges, which experienced a maximum uplift of 0.004 in (0.1 mm).

Figure 19 shows the stress and strain contours for the ASLE. A maximum stress of 1 lbf/in² (6.9 kN/m²) and a maximum strain of 0.0008 in/in (0.0021 cm/cm) underneath the right anchor near the load is observed. The analytical investigations indicated a maximum deflection of 0.011 in (0.28 mm) at the right edge of the centerline near the load and no serious uplift. Only the far left edge is lifted; the maximum uplift is 0.001 in (0.03 mm). the central anchors carry 23 percent less load than the right anchors do, whereas the left anchors carry 49 percent less load than the right anchors do.

COMPARISON OF EXPERIMENTAL AND ANALYTICAL SOLUTIONS

A comparison of the analytical solution with the experimental results is shown in Figures 20, 21, and 22. Figure 20 shows the deflection of the SL along the transverse centerline T1-R1 for a 750-lb load at position 1. The difference is about 20 percent. The experimental program on the SL was conducted after the loading for the ASL and the ASLE had been completed. A number of loadings and unloadings do strengthen the soil, and this is probably one of the major factors that contributes to the difference between the experimental and the analytical values.

In Figure 21, the transverse and longitudinal centerline surface deflections of the finite-element

Figure 22. Transverse and longitudinal surface deflections along lines T1-R1 and L2-N2, load position 1, for ASLE.

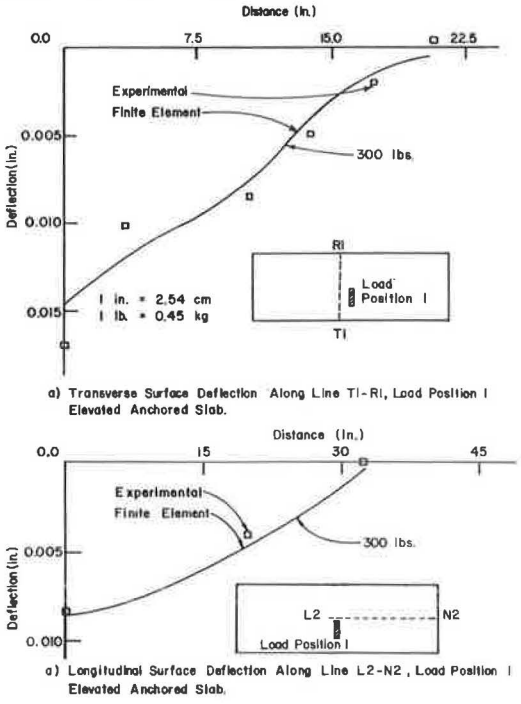

model of the ASL for a 750-lb load are plotted as well as the experimentally observed points. The difference is about 11 percent. Figure 22 presents the transverse and longitudinal deflections and the experimental points for the ASLE for a 300-lb load at position 1. Although the longitudinal deflections show remarkable agreement, there is a difference of about 18 percent between observed and analytical values for the transverse deflections.

Although every effort was made to maintain the uniformity of the subgrade, human factors do cause nonuniformities. Keeping these factors in mind, it may be remarked that, in general, the trends of observed deflection of the model tests agree well with the analytical (finite-element) results. Although the paper presents results of only a few of the many experiments conducted, the inferences are based on a study of all experimental results.

CONCLUSIONS

The anchored slab offers two distinct advantages over the conventional slab. First, deflections are lower and more uniform. Second, stress in the soil is lower and distributed more widely by the rigid anchors. A significant portion of the pavement-distress mechanism arises from the subgrade, in which the soil is under greater confining stress (and as a result is stronger), and when moisture and temperature fluctuations are not acute, subgrade-related failure is less likely to occur.

REFERENCES

1. S.K. Saxena, J.W.H. Wang, J.J. Udwari, and W.J. Rosenkranz. Unique Concepts and Systems for Zero-Maintenance Pavements. FHWA, U.S. Department of Transportation, Rept. FHWA/RD-77-76, July 1977.
2. L.W. Teller and E.C. Sutherland. The Structural Design of Concrete Pavements. Public Roads, Vol. 16, Nos. 8 and 9, 1935, pp. 145-158, 169-197; Vol. 16, No. 10, 1935, pp. 201, 221; Vol. 23, No. 8, 1943, pp. 167-212.
3. M.G. Spangler. Stresses in Concrete Pavement Slabs. Proc., HRB, Vol. 15, 1935, pp. 122-146.
4. C. Vander Veen. Loading Tests on Concrete Slabs at Schiphol Airport. Proc., 3rd International Conference on Soil Mechanics and Foundation Engineering, Switzerland, 1953, pp. 133-141.
5. S.K. Saxena and A.S. Vesic. Experimental Study of Slabs Resting on a Silty Clay Subgrade. Presented at the 57th Annual Meeting, HRB, 1978.
6. S.K. Saxena, J. Hedberg, and C.C. Ladd. Geotechnical Properties of Varved Clays of Hackensack Meadow, N.J., U.S.A. ASTM Geotechnical Testing Journal, Vol. 1, No. 3, Sept. 1978.
7. T.H. Wu. Retaining Walls. In Foundation Engineering Handbook, Van Nostrand Reinhold, New York, 1975.
8. S.K. Saxena, W.J. Rosenkranz, and S.G. Militsopoulos. New Structural Systems for Zero-Maintenance Pavements, Volume 1--Analytical and Experimental Studies of an Anchored Pavement: A Candidate Zero-Maintenance Pavement. FHWA, U.S. Department of Transportation, Rept. FHWA/RD-80-026, May 1980.
9. M.G. Spangler and F.E. Lightburn. Stresses in Concrete Pavement Slabs. Proc., HRB, Vol. 17, 1937, pp. 215-234.

Publication of this paper sponsored by Committee on Rigid Pavement Design.

Prestressed Concrete Overlay at O'Hare International Airport: In-Service Evaluation

DONALD M. ARNTZEN

A 240-m (800-ft) prestressed concrete overlay was placed on the 27L end of runway 9R-27L at Chicago O'Hare International Airport. The overlay consisted of two 120 x 46-m (400 x 150-ft) sections 20 or 23 cm (8 or 9 in) thick. The pavement was posttensioned by using a fully bonded bar system. Conventional paving and tensioning equipment was used, and the cost and time of construction were comparable with those of conventional paving systems of portland cement concrete.

At 10:00 a.m., Sunday, August 24, 1980, runway 27L at Chicago O'Hare International Airport was reopened for traffic after completion of a prestressed concrete overlay. This overlay of the threshold 240 m (800 ft) long was another step in the ongoing program to rehabilitate and upgrade the airfield pavement system.